

## **Inversion and Prediction-Focused Approach (PFA) imaging of multiple loops Surface Nuclear Magnetic Resonance (SNMR) data**

**Auteur :** Michel, Hadrien

**Promoteur(s) :** Nguyen, Frederic

**Faculté :** Faculté des Sciences appliquées

**Diplôme :** Master en ingénieur civil des mines et géologue, à finalité spécialisée en géologie de l'ingénieur et de l'environnement

**Année académique :** 2017-2018

**URI/URL :** <http://hdl.handle.net/2268.2/4549>

---

*Avertissement à l'attention des usagers :*

*Tous les documents placés en accès ouvert sur le site le site MatheO sont protégés par le droit d'auteur. Conformément aux principes énoncés par la "Budapest Open Access Initiative"(BOAI, 2002), l'utilisateur du site peut lire, télécharger, copier, transmettre, imprimer, chercher ou faire un lien vers le texte intégral de ces documents, les disséquer pour les indexer, s'en servir de données pour un logiciel, ou s'en servir à toute autre fin légale (ou prévue par la réglementation relative au droit d'auteur). Toute utilisation du document à des fins commerciales est strictement interdite.*

*Par ailleurs, l'utilisateur s'engage à respecter les droits moraux de l'auteur, principalement le droit à l'intégrité de l'oeuvre et le droit de paternité et ce dans toute utilisation que l'utilisateur entreprend. Ainsi, à titre d'exemple, lorsqu'il reproduira un document par extrait ou dans son intégralité, l'utilisateur citera de manière complète les sources telles que mentionnées ci-dessus. Toute utilisation non explicitement autorisée ci-avant (telle que par exemple, la modification du document ou son résumé) nécessite l'autorisation préalable et expresse des auteurs ou de leurs ayants droit.*

---

# Appendix C

## Deterministic inversion: Resolution matrices

A way to assess the ability of the model to retrieve correct data in a deterministic way is to compute the associated resolution matrix. To do so, Müller-Petke and Yaramanci proposed in 2008 an approach based on the singular-value decomposition (SVD) of the forward operator:

$$\mathbf{d}^{\text{obs}} = \mathbf{G}\mathbf{m} = \mathbf{U}\mathbf{S}\mathbf{V}^T \mathbf{m} \quad (\text{C.1})$$

They suggested the use of the Picard conditions (linked to Picard plots) to assess the right truncation to apply to the decomposed problem in order to avoid noise propagation in the model. The use of the Picard condition is supposed to account for the noise level and avoid noise propagation, similarly to regularization parameters in the QT inversion (Müller-Petke & Yaramanci, 2008). It states that the value of :

$$a_i = |\mathbf{u}_i^T \mathbf{d}| / \sigma_i \quad (\text{C.2})$$

where,

- $\mathbf{u}_i^T$  is the transpose of the  $i^{\text{th}}$  column of the matrix  $\mathbf{U}$
- $\mathbf{d}$  is the data (here, the amplitude at  $t=0$  to comply with the linearity of the problem)
- $\sigma_i$  is the  $i^{\text{th}}$  singular value (diagonal of  $\mathbf{S}$ )

should remain more or less constant or decrease with the value of the index  $i$  (Fedi, Hansen, & Paoletti, 2005).

From the Picard plot, it is possible to establish a reasonable truncation. In this work, it has been chosen to use a simple algorithm to compute the "best" truncation index:

1. Compute the means of the  $a_i$  values from  $i - 10$  to  $i$
2. Compute the relative increment of each mean value
3. Find the first relative increment larger than 25%

Then, the resolution matrices were computed using:

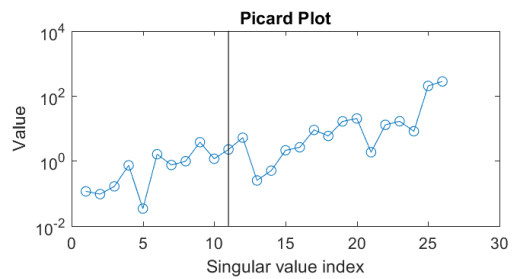
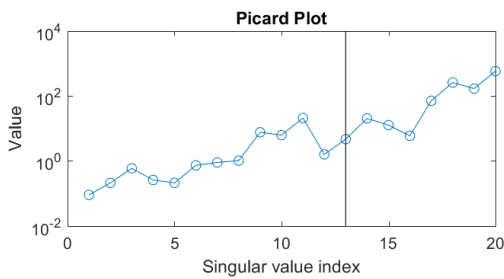
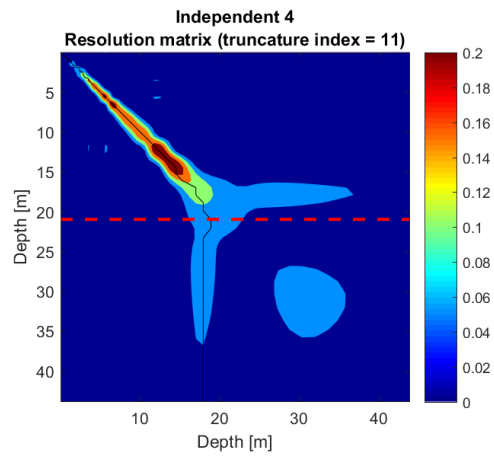
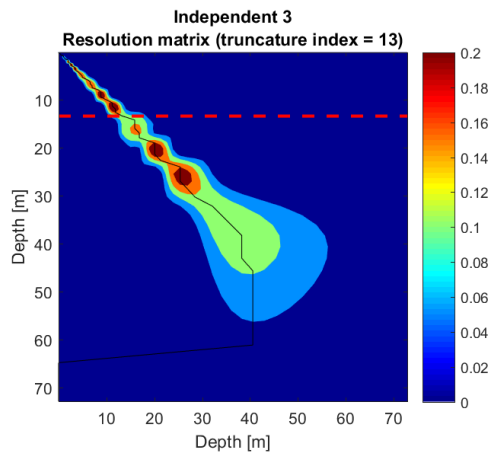
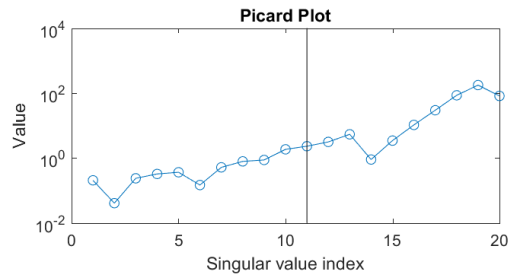
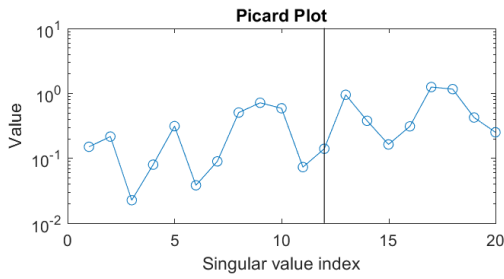
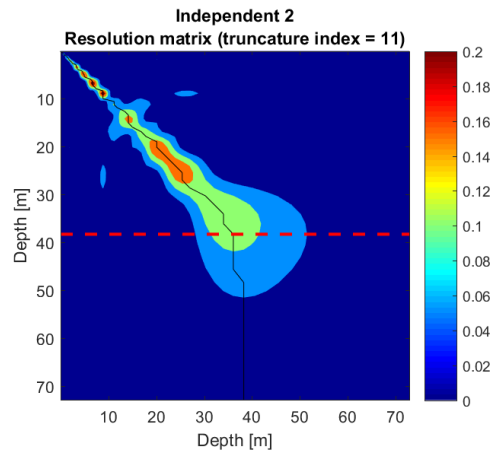
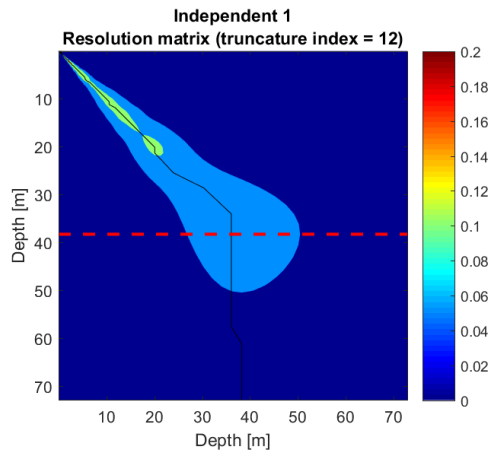
$$\mathbf{R}_m = \mathbf{V}_p \mathbf{V}_p^T \quad (\text{C.3})$$

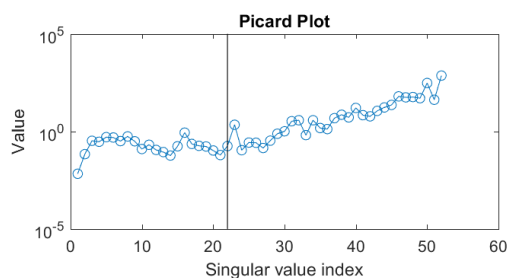
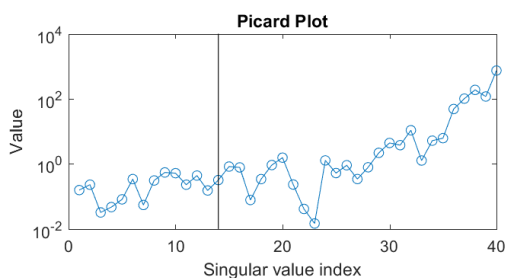
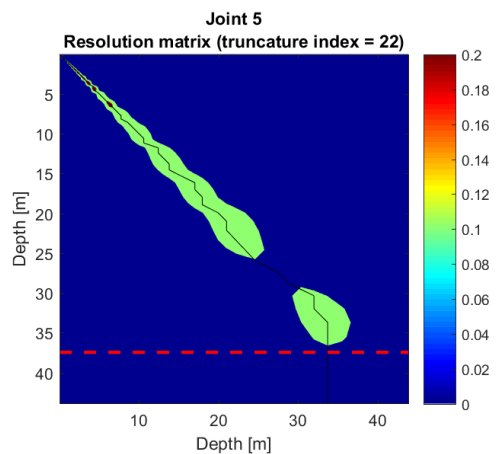
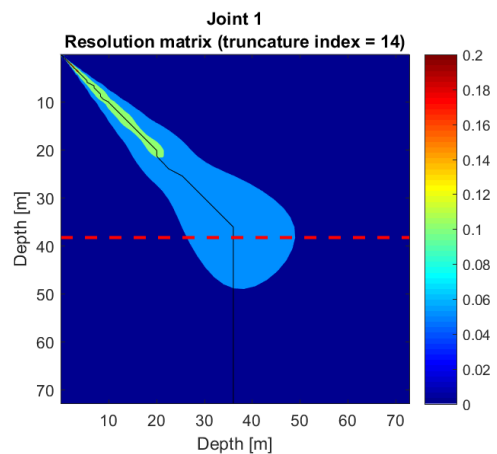
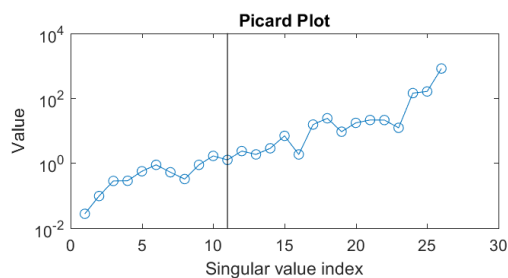
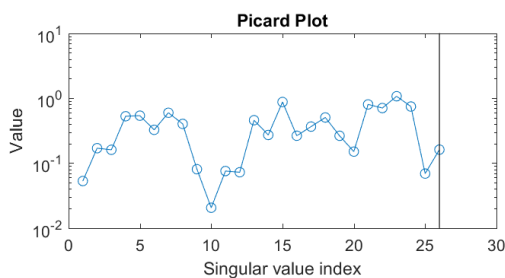
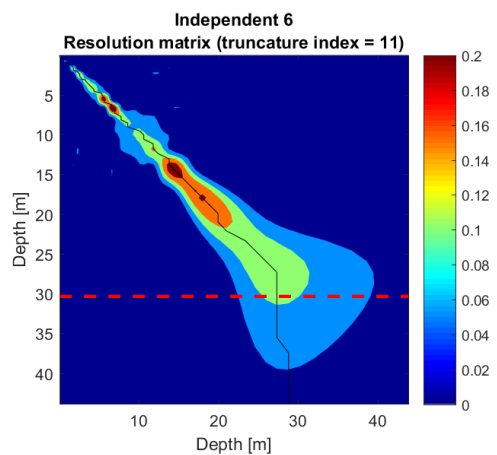
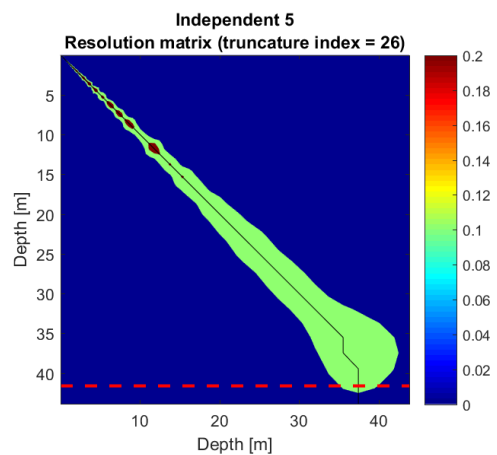
with  $p$ , the truncation index ( $\mathbf{V}_p$  is the matrix constituted of the  $p$  first columns of the  $\mathbf{V}$  matrix from the SVD) (Müller-Petke & Yaramanci, 2008).

This process has been applied to all the inversions presented in the Subsection 7.3.2 (Chapter 7). The results of such analyses are presented in Figure C.1.

From those matrices, it is interesting to point out that the "Independent 1" and "Independent 5" datasets (hence the same transmitter/receiver) are producing the clearest resolution matrices with a very narrow resolution at the top and a spreading with depth. The other inversions are susceptible to a larger spreading of the resolution, even at low depth. However, the "depth of confidence", marked with the dashed red line, is changing with the type of transmitter/receiver couple in the "Independent" inversions, whereas this depth is not significantly changing with the "Joint" and "General" inversions. The use of the "Joint" and, to a larger extent, the "General" inversions tends to decrease the spreading of the resolution matrix along the diagonal, hence to recover the behavior of the classical inversions.

The use of the 10 m loop is also questionable from the analysis of the observation of the resolution matrices. Actually, it seems that the corresponding "Independent 3" and "Independent 6" are the ones that lead to smaller confidence depths (respectively 13.5 and 30.5 m) compared to the classical inversions. It is also observed that the "Independent 4" (30 m transmitter but 50 m receiver) resolution matrix has a large spreading around 20 m, which limits the confidence depth to 21.0 m. However, contrary to the two other limited resolution cases, the resolution of this model shows very few spreading around the diagonal above this confidence depth, which ensures a better model.





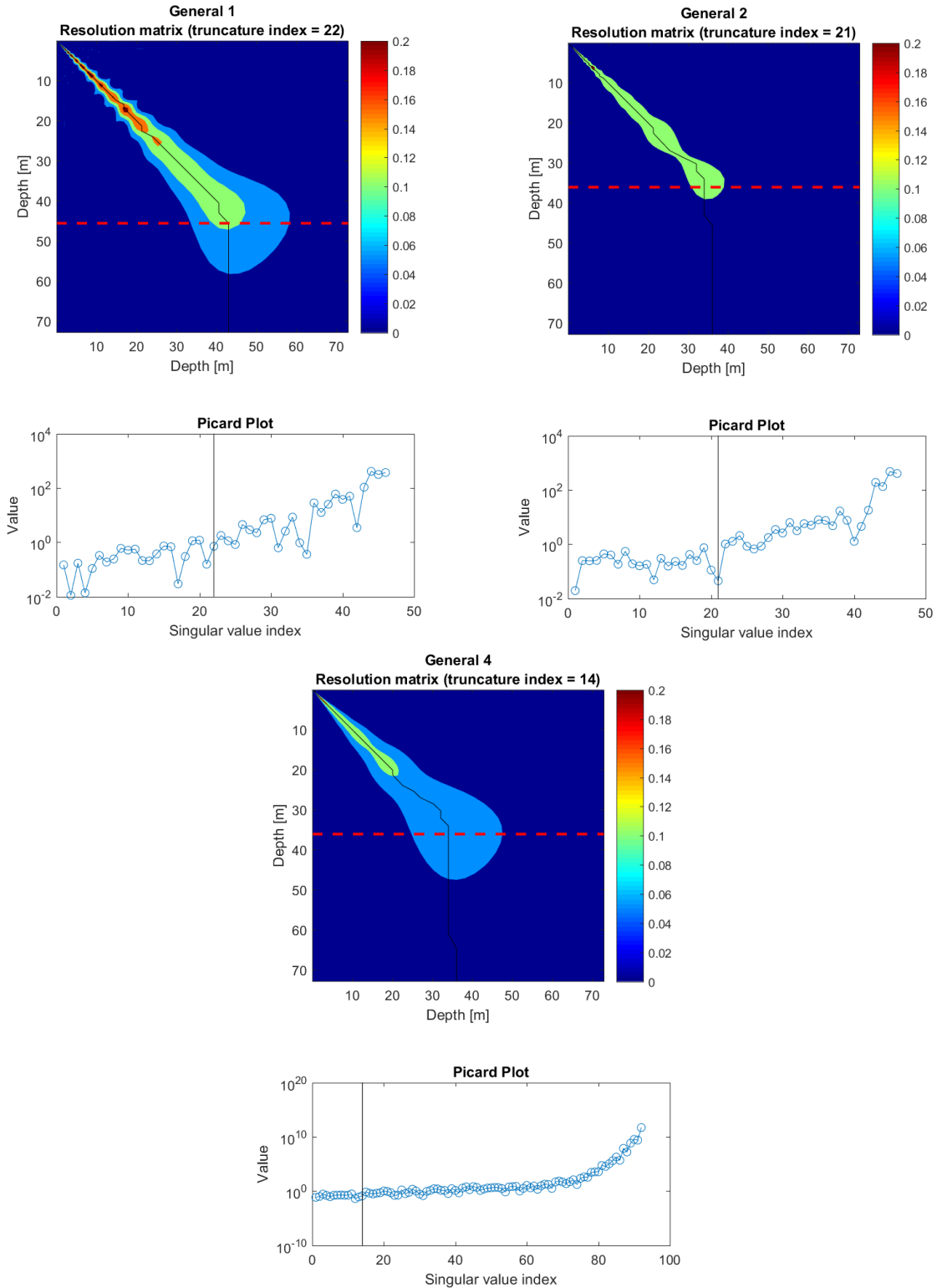


Figure C.1: Resolution matrices (absolute value) and Picard plots for the different inversions proposed in the Subsection 7.3.2. The black line represents the maximum of resolution and the dashed red line represents the maximal depth where the deviation from the diagonal is less than 10% (Müller-Petke & Yaramanci, 2008).